Heliyon 5 (2019) e01912

Contents lists available at ScienceDirect

Heliyon

journal homepage: www.heliyon.com

Enhanced photocatalytic activity against crystal violet dye of Co and In doped ZnO thin films grown on PEI flexible substrate under UV and sunlight irradiations

S. Ben Ameur [a], H. BelHadjltaief [b], B. Duponchel [c], G. Leroy [d], M. Amlouk [e], H. Guermazi [a,*], S. Guermazi [a]

[a] Research Unit: Physics of Insulators and Semi Insulator Materials, Faculty of Science of Sfax, Road of Soukra Km 3.5, B.P:1171, 3000, Sfax, University of Sfax, Tunisia
[b] Laboratory of Eau, Energie et Environnement, National Engineering School of Sfax, B.P1173.W.3038, Sfax, University of Sfax, Tunisia
[c] UDSMM, University Lille North of France, ULCO, 59140, Dunkerque, France
[d] UDSMM, University Lille North of France, ULCO, 62228, Calais, France
[e] Research Unit: Physics of Semi-conductor Devices, Faculty of Science of Tunis, Tunis El Manar University, 2092, Tunis, Tunisia

ARTICLE INFO

Keywords:
Materials science
Nanotechnology
Materials testing
Nanostructured material
ZnO thin films
Flexible substrate
Crystal violet dye
Photocatalysis
Photostability

ABSTRACT

This work is focused on the photocatalytic activities of undoped ZnO, Co (1%) doped ZnO (CZO) and In (1%) doped ZnO (IZO) thin films grown on flexible PEI (Polyetherimide) substrate by spray pyrolysis. The photodegradation of crystal violet dye was investigated under UV and sunlight irradiations. Doping and excitation energy effects on photocatalytic efficiencies are discussed. All ZnO thin films show high photocatalytic efficiency up to 80% under either UV or sunlight irradiations for 210 min. However, CZO has the higher photocatalytic performance under UV irradiation. While, the photodegradation efficiency of IZO was enhanced under sunlight irradiation due to the narrowing of its optical gap. These results are discussed based on structural, morphological and optical investigations. The photocatalytic stability of ZnO films was studied as well. So, after three photocatalysis cycles, all ZnO thin films still effective. The obtained results are promising for the use of doped ZnO/PEI as talented photocatalysts for applications in large surfaces with various geometries for photodegradation of hazardous pollutants.

1. Introduction

In recent decades, water purification becomes one of the popular environmental challenges. Organic dyes are the major class of pollutants in the wastewater coming from textile, paper printing, and plastic manufacturing processes. Photocatalysis is a promising approach in regard to the removal processes of these pollutants [1, 2, 3]. Notably, the use of the semiconductors as photocatalysts is one of the wide interest axes to resolve environmental pollution problems [4, 5]. A various semiconductor such as TiO_2, ZnO, and SnO_2 [6, 7, 8, 9, 10] are presented as promising photocatalysts. TiO_2 is the most applied one [11, 12]. However, ZnO has been proposed as an alternative photocatalyst to TiO_2 since it has been found to be more economic [13] safe and biocompatible for most environmental applications [6, 14]. In addition, it exhibits higher absorption efficiency across a large fraction of the solar spectrum when compared to TiO_2 [15]. Many researchers reported on the use of ZnO powder for the photocatalytic activity [16, 17, 18, 19, 20]. However, more attention has been focused on the use of thin films [21, 22, 23] to overcome several practical problems arising from the use of powder such as the difficulty separating the insoluble catalyst from the suspension, as well as recycling of the catalyst powders. The photocatalytic activities of ZnO thin films deposited on a glass substrate and on flexible polymer substrate have been reported [24, 25]. However, the photocatalytic performance of ZnO thin films deposited on other substrates is somewhat studied. In addition, Alessandro Di Mauro et al [26] reported that ZnO thin films deposited on PMMA flexible substrate have a comparable photocatalytic activity to the ZnO film deposited on Si substrate under UV light irradiation. Thus, we are interested in the use of ZnO thin films, grown on flexible PEI (Polyetherimide) substrate as photocatalysts [27, 28], since PEI has better mechanical properties compared to glasses. This makes the elaborated photocatalysts suitable to be used in various geometries.

* Corresponding author.
E-mail address: hajer.guermazi@gmail.com (H. Guermazi).

https://doi.org/10.1016/j.heliyon.2019.e01912
Received 4 January 2019; Received in revised form 23 February 2019; Accepted 3 June 2019

Furthermore, introduced impurity levels by doping with various elements such as Cu [29], Fe [30], Ni [31], Co [32], C [33] and In [34] generated lattice defects can have a significant influence on the photocatalytic performance of materials.

In previous work [35], it is found that doping ZnO thin films by Co, or In changed its physical properties. Hence, in this work, our research efforts are focused on the investigation of the effect of Cobalt and Indium doping on the photocatalytic efficiency of ZnO films deposited on a flexible substrate. The photocatalytic activities were tested for degradation of crystal violet under UV and sunlight irradiations in similar experimental conditions. The photocatalytic stability of the studied films is investigated as well. All obtained results are correlated and the enhanced photocatalytic activity is interpreted based on structural, morphological and optical investigations.

2. Experimental

2.1. Preparation of ZnO thin films and characterization techniques

ZnO, IZO (In (1%) doped ZnO) and CZO (Co (1%) doped ZnO) were grown by the spray pyrolysis technique on PEI substrate at T = 250 °C. We used zinc acetate dihydrate (Zn $(CH_3COO)_2$. $2H_2O$) dissolved in distilled water and propanol mixture [36]. The doping sources are $CoCl_2$ and $InCl_3$for Co and In respectively with 1% doping percentage. More details were reported in previous work [35].

The structural characterization is carried out by X-ray diffractometer (Analytical X Pert PROMPT). Cukα radiation (λ = 1.5406Å) was used as an excitation source. The morphological properties are studied by AFM spectroscopy. The optical parameters were determined using a Shimadzu UV 3100 UV-Vis-NIR spectrophotometer in the wavelength range from 300 to 2000 nm. As well, PL measurements are carried out at room temperature using Perkin Elmer LS-55 Luminescence/Fluorescence spectrophotometer with 325 nm as a wavelength excitation.

2.2. Photocatalysis test

The photocatalytic activity was checked in the process of Crystal violet (CV) photodegradation with an initial concentration of C_0 = 12.5 mg/L. The irradiation was carried out using an UV-lamp (Black-Ray B 100WUV-lamp, V-100AP series) with a wavelength of 365 nm and sunlight irradiation. Before illumination, the dispersion was magnetically stirred for 60 min (in the dark), in order to ensure an adsorption equilibrium between the sample surface and the organic dye [37]. The photodegradation duration is chosen equal to 210 min. A detailed description of the photocatalytic reactor was reported in earlier studies [27, 38].

The concentration of CV was measured by a UV-Visible spectrophotometer (Shimadzu UV-vis spectrophotometer model 160A). Therefore, the CV dye photodegradation efficiency (η) was calculated at the maximal absorption wavelength of CV solution λ_{max} = 578 nm as follows [39]:

$$\eta(\%) = \left(1 - \frac{C}{C_0}\right) \times 100 \quad (1)$$

where C is the actual dye concentration of CV at time t of the reaction and C_0 is the initial dye concentration and $C/C_0 = A/A_0$ (A is the absorbance of the CV dye solution).

3. Results and discussions

3.1. Physical investigations

Fig. 1 shows the XRD patterns of ZnO, IZO (In (1%) doped ZnO) and CZO (Co (1%) doped ZnO) thin films, as well as PEI substrate. The diffraction peaks matched well the hexagonal wurtzite structure of ZnO

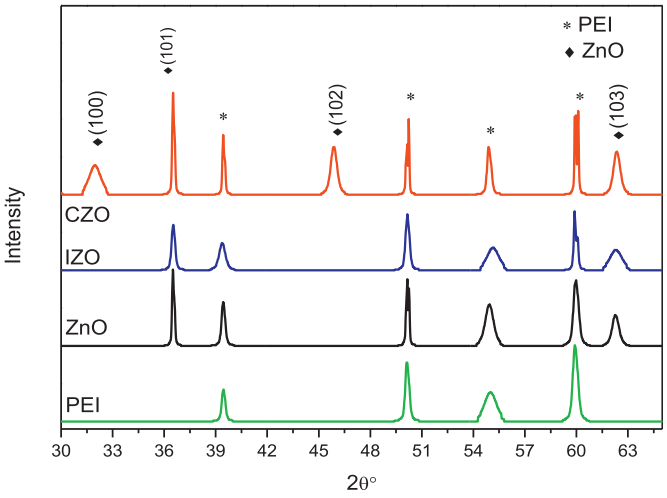

Fig. 1. XRD patterns of ZnO, IZO, CZO thin films and PEI substrate.

according to the (JCPDS 36–1451) with (101) preferred orientation. Besides, XRD spectra revealed the presence of peaks corresponding to the PEI substrate.

The lattice parameters a and c for ZnO/PEI thin films were calculated from the XRD patterns by using the following equation:

$$d_{hkl} = \left(\frac{4}{3}\frac{h^2 + hk + k^2}{a^2} + \frac{l^2}{c^2}\right)^{-\frac{1}{2}} \quad (2)$$

where h, k, and l are the Miller indices of the planes and d_{hkl} are the interplanar spacing.

The lattice parameters, computed using Eq. (2), are shown in Table 1. By comparing the obtained values with the standard lattice volume, we can note that CZO film has the volume closer to that of bulk ZnO. Thus, it seems the most relaxed lattice. This means an improvement in the crystalline quality of films, and indicates the substitution of Zn^{2+} by Co^{2+} ions [40, 41, 42]. In fact, since the ionic radius of Co^{2+} (0.072 nm) is close to that of Zn^{2+} (0.074 nm); it presents large solubility in the ZnO matrix [43].

Furthermore, from XRD patterns, we can determine the microstructural parameters such as the crystallite size (D), the micro-strain (ζ) and the dislocation density (δ) using the following expressions (3–5) [44]:

$$D = \frac{0,9\lambda}{\beta \cos\theta} \quad (3)$$

$$\delta = \frac{1}{D^2} \quad (4)$$

$$\xi = \frac{\beta}{4\tan(\theta)} \quad (5)$$

Table 1
XRD parameters of undoped and doped ZnO thin films deposited on PEI substrate.

	ZnO	IZO	*CZO*
a(Å)	3.247	3.249	3.257
c(Å)	5.200	5.201	5.214
V(Å^3)	46.600	46.666	47.014
D (nm)	83.3	41.7	83.4
δ (10^{-4}nm^{-2})	1.44	5.76	1.44
ζ (10^{-4})	13	27	13
S (m^{2}g^{-1})	0.124	0.248	0.124
RMS (nm)	20,4	6.9	20.5

a_0=b_0= 3.249 (Å), c_0= 5.206 (Å) and V_0= 47.63 (Å^3) From JCPDS 36-1451.

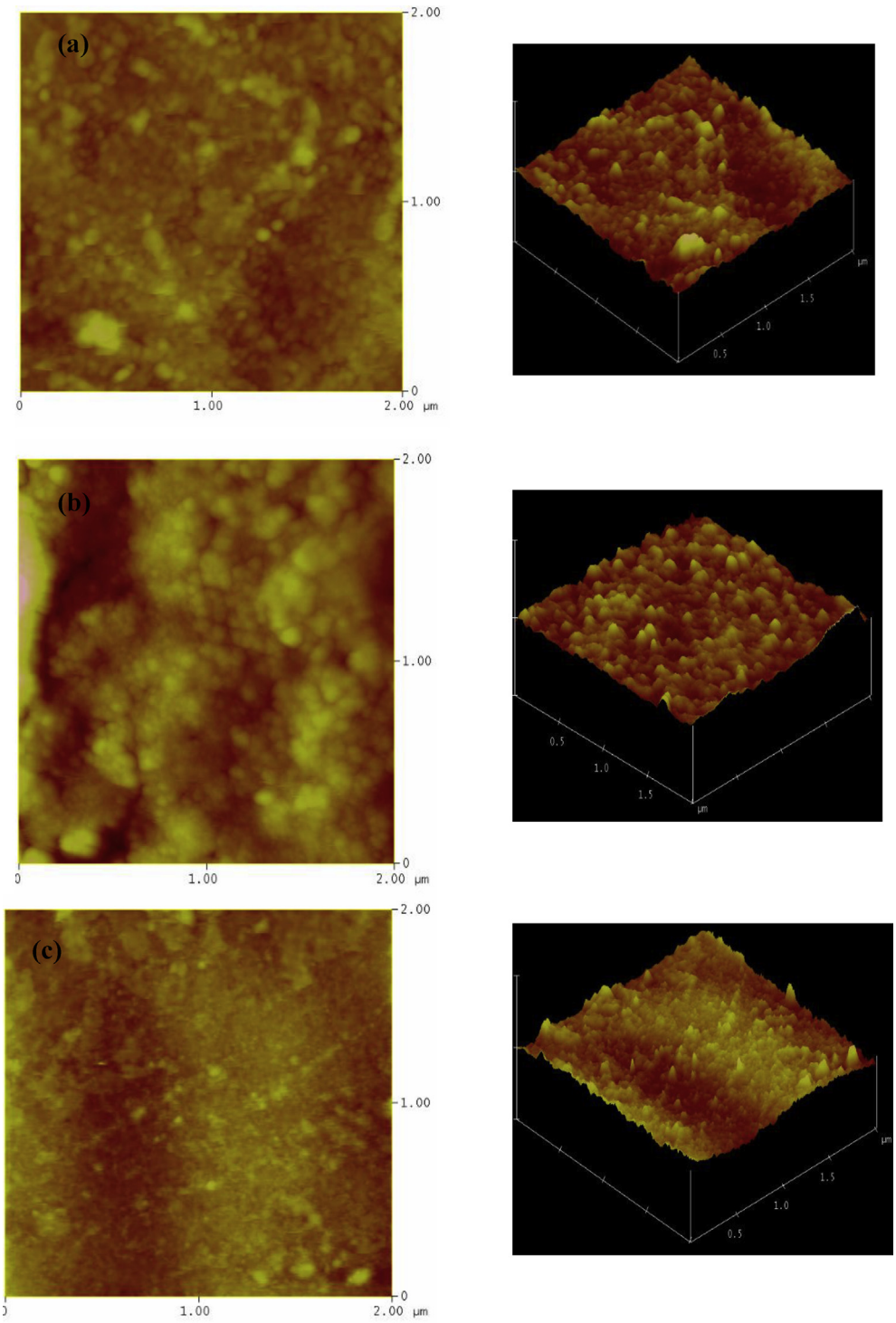

Fig. 2. 2D and 3D topographic AFM images of ZnO films:(a)ZnO,(b) CZO and (c) IZO.

The obtained values show that the crystallite size (D) (Table 1) is not affected by doping with Co. This is probably due to the substitution between Co^{2+} ions and Zn^{2+} ions in ZnO lattice [45]. Moreover, for IZO films the crystallite size decreases, this is can be explained by the incorporation of In^{3+} ions in the interstitial sites of the ZnO lattice [46]. This hypothesis can be supported by the high microstrain (ζ) value (27.10^{-4}), calculated from (Eq. (5)).

Assuming that the particles have a spherical shape, we can estimate the specific surface area from the crystallite size, using formula (6 and 7) [47]:

$$S = \frac{6}{D\rho} \tag{6}$$

$$\rho = \frac{nM}{NV} \tag{7}$$

where ρ is the density of the particles, M is the molar weight of substance (M = 81.38 g/mol), n is the number of formula units in the unit cell (n = 2 for ZnO according to the JCPDS 36–1451 card), V is the volume of the unit cell, and N is Avogadro's number.

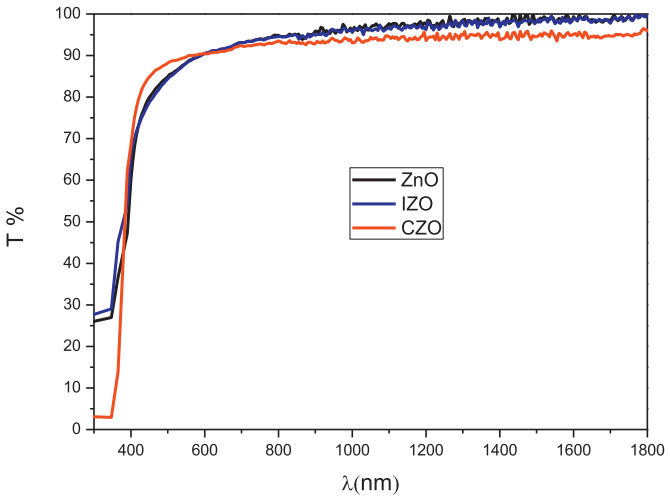

Fig. 3. Transmittance spectra of ZnO, CZO, IZO thin films.

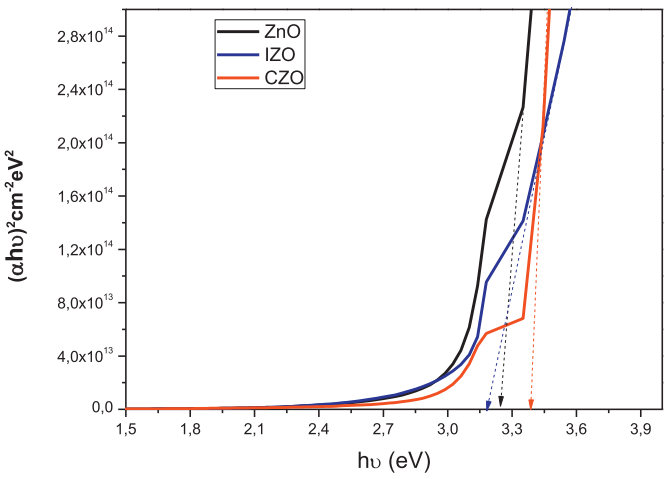

Fig. 4. Optical band gap energy estimation of ZnO, IZO and CZO thin films.

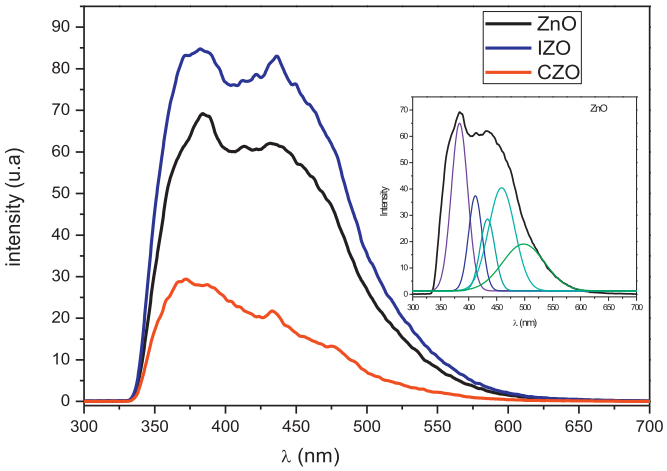

Fig. 5. PL spectra of all ZnO thin films and deconvolution of undoped ZnO spectra as an example (inset).

The obtained specific surface area values are listed in Table 1. The values show that the IZO has the larger specific surface area, which is promising to high photocatalytic efficiency. This will be confirmed in the following sections.

The presence of defects due to various elements doping will affect the morphological and optical properties of ZnO thin films. In particular, the change of crystallite size and lattice strain will have a profound impact on the PL spectra of ZnO thin films, which will be discussed later.

The surface morphology of all deposited ZnO thin films was estimated by AFM. This study gives information about the surface topography and the average roughness (RMS) values. Notably, the photocatalytic activities of thin films depend on surface roughness.

Fig. 2 shows 3D and 2D topographic views of all films (2 × 2μm). From images especially 3D, it can be seen that all film surfaces are rough, whereas IZO surface is the smoother one. CZO thin films have densely packed grains dispirited on all surface with hollow zones showing rough surface. The RMS values are found to range between 6.9 nm and 20.5 nm (Table 1). As can be seen, the introduction of indium on the ZnO lattice causes a decrease of surface roughness up to 6.9 nm. This is related to the average crystallite size.

Using a UV–Vis–NIR spectrometry, we can study the optical properties of the ZnO films in the wavelength range from 300 to 1800 nm. The transmittance spectra of ZnO, IZO and CZO thin films are shown in Fig. 3. All films are absorbers in the UV region and they exhibit a high transmission (T (%) ≥ 85%) in visible and NIR regions (400–1800 nm). Such transparency may be due to low scattering and absorption losses. The elaborated ZnO thin films exhibit sharp absorption edges in the ultraviolet region (360–400 nm). From this region, we can determine the optical band gap values using Tauc's relation (Eq. (8)) for allowed direct transitions [48]:

$$(\alpha h\nu)^2 = A\left(h\nu - E_g\right) \tag{8}$$

The optical band gap energy was calculated by extrapolation of the linear part of $(\alpha h\nu)^2$ vs hν plot, as shown in Fig. 4. The obtained gap energy values are 3.22, 3.33 and 3.18 eV for undoped ZnO, CZO and IZO thin films respectively.

The photoluminescence spectroscopy was used to deduce the photo-active centers in ZnO thin films. These photo-active centers are really the defects whose affect the electron-hole recombination. So, Controlling of intrinsic defects is of paramount importance in applications of ZnO.

The PL spectra of ZnO, IZO and CZO thin films, measured at room temperature with an excitation wavelength of 325 nm, were shown in Fig. 5. Firstly, we note a decrease of PL intensity after doping with Co which indicates that CZO thin film has low electron-holes recombination rate, thus it may exhibit better photocatalytic activity than ZnO and IZO ones.

As can be seen in all ZnO thin films, the emission is mainly categorized as near band edge emission in the UV region and some emissions in the visible range. Usually, ZnO has six kinds of defects, namely oxygen vacancies (V_O), oxygen interstitials (O_i), oxygen antisites (Zn_O), zinc vacancies (V_{Zn}), zinc interstitials (Zn_i), and zinc antisites (O_{Zn}) [49]. From the deconvolution using Gaussian analysis, shown in the inset of Fig. 5, we can determine the different defects energy states. The photoluminescence (PL) spectra of all ZnO thin films, typically show emission bands in the ultraviolet (UV) and visible (violet, blue, blue-green- and green) regions. Firstly, the UV emission is usually considered as the

Table 2
Charachetreistics of photoluminescence peaks: positions and energy.

		ZnO	IZO	CZO
Peak 1	Position (nm)	383	385	366/390
UV	Energy (eV)	3.239	3.222	3.39/3.18
Peak 2	Position (nm)	412	408	411
Violet	Energy (eV)	3.011	3.04	3.018
Peak 3	Position (nm)	432/460	430/462	430/463
Blue	Energy (eV)	2.871/ 2.697	2.885/ 2.685	2.885/ 2.68
Peak 4 blue- Green	Position (nm)	495	504	-
	Energy (eV)	2.51	2.461	
Peak 5	Position (nm)	-	564	526
Green	Energy (eV)		2.22	2.358

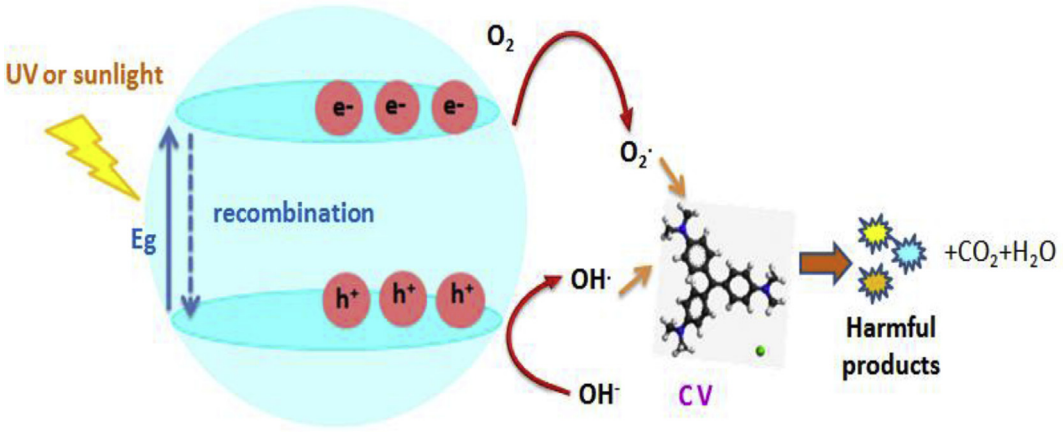

Fig. 6. Photocatalytic process of CV degradation using ZnO catalysts.

characteristic emission of ZnO [50] and attributed to the near band–edge transition or excitonic recombination.

It is suggested that the origin of the violet emission at λ ~410 nm (3.02 eV) is due to the transitions from conduction band (CB) to the holes localized at defect level associated with zinc vacancy (V_{Zn}) [51]. The blue luminescence bands situated in (430–480) nm (2.8–2.68 eV) domain are due to transitions from extended donor Zn_i states and the holes in the valence band [52]. The blue-green emissions [480–510 nm] may be due to the transition from the oxygen inertial (O_i) and zinc antisites (O_{Zn}) to the valence band [53]. The visible green emissions peaks located at λ > 520 nm are observed only for CZO and IZO thin films (Table 2). This emission has been widely reported as oxygen vacancies. Therefore, the doping element causes a loss of oxygen and thus the formation of oxygen vacancies (V_O). Furthermore, intrinsic oxygen non-stoichiometry leads to the presence of a large number of oxygen defect sites in doped ZnO surface which may serve as electron trapping sites making it suitable for efficient photocatalytic applications [54, 55, 56].

3.2. Photocatalytic activities

The photocatalytic activities of all ZnO thin films are evaluated by the Crystal violet (CV) photodegradation under UV and sunlight irradiations for 210 min. The principle of photocatalysis is the irradiation of ZnO with energy equal to or higher than the energy band gap, which causes promotion of an electron from the valence band (VB) to the conduction band (CB). The combination of the positive hole (h^+) with water and/or hydrogen peroxide (H_2O_2) produces hydroxyl radicals (•OH). Simultaneously, oxygen molecules absorbed on the photocatalyst are reduced by the electrons in the conduction band, and produce a superoxide radical anion ($O_2^{\bullet-}$) [57, 58]. The generated •OH and $O_2^{\bullet-}$ are all powerful oxidant for the degradation of organic compounds. Incorporation of doping ions into ZnO lattice will create more electrons and holes traps, which fasten the charge carriers and thus suppress the recombination of photoinduced electrons and holes, leading to the improvement of the photocatalytic activity [59, 60]. The mechanism is more detailed in Fig. 6.

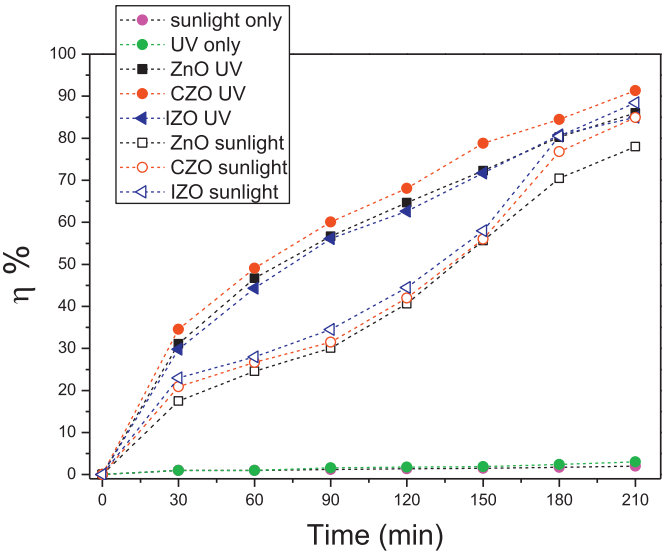

Fig. 7. The photodegradation efficiency of undoped and (In, Co) doped ZnO thin films under UV and sunlight irradiations.

The photodegradation efficiency, computed from Eq. (1), was plotted versus the irradiation time, for ZnO thin films under UV and sunlight irradiations (Fig. 7). Firstly, preliminary experiments were carried out without photocatalysts, the CV solution was exposed to UV or sunlight irradiation. The results show that the photodegradation efficiencies are around (3%) and (2%) for UV and sunlight irradiation, respectively. Insignificant degradation was observed. On the one hand, we note that ZnO thin films under UV and sunlight have different photocatalytic activities. Under UV irradiation after 210 min, the photodegradation efficiency is 86%, 91.3% and 85% for ZnO, CZO and IZO, respectively. However, after the same time under sunlight irradiation, the photodegradation efficiency is 78%, 85% and 88.5% for ZnO, CZO and IZO, respectively.

In general, the photocatalytic activity was sensitive to the crystalline, surface OH groups, specific surface area and the roughness of the photocatalyst surface. Hence, the CZO has the higher photocatalytic performance under UV irradiation. This result can be attributed to the position of dopants into the ZnO lattice. As demonstrated by DRX, the Co^{2+} substituted Zn^{2+} whereas the In^{3+} is localized on the interstitial site which causes crystal defects. Many results [30,60] approve that the dopants localized in interstitial sites would act as trapping or recombination centers for photo-excited electrons and holes [55]. Furthermore, it causes a slight decrease in the photocatalytic activity as seen in IZO thin films. Besides, some works of literature [61,62] have already reported that smaller grain size has a higher-population of surface defects for the enhanced defect emission relative to PL emission. Indeed, we have noticed an obvious enhancement in PL emission in IZO. Additionally, the concentration of defects on the surface of the catalyst can also make a difference in photocatalytic activity [63]. Moreover, CZO film has a good crystallinity combined with a high surface roughness, which improves its photocatalytic performance compared to ZnO and IZO ones [64]. This enables sample absorption in the visible range of the solar spectrum [39]. In addition, IZO has the largest specific area. This result reveals that all

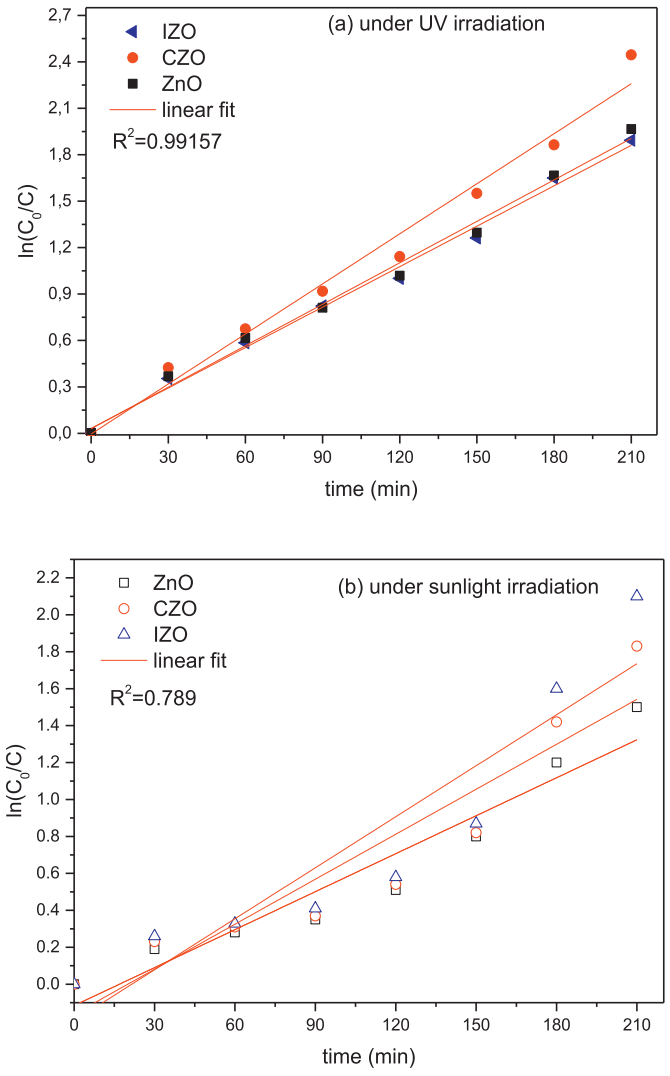

Fig. 8. Plot of $\ln\left(\frac{C_0}{C}\right)$ versus irradiation time for ZnO, CZO and IZO thin films, under (a) UV and (b) sunlight irradiation.

ZnO thin films show promising photocatalytic activities under UV as well as visible light comparable to ZnO thin films deposited on glass substrate.

On the other hand, Fig. 7 shows a difference in photodegradation kinetics of CV degradation using undoped and (Co, In) doped ZnO thin films. Furthermore, it is ordered to quantify the photodegradation kinetics of the CV; we used the formula of a pseudo first order process studied by Langmuir and Hishelwood. It is reported [17] that the rate of photocatalysis of CV dye by irradiated ZnO thin films was investigated via pseudo-first-order kinetics (Fig. 8):

$$\ln\left(\frac{C_0}{C}\right) = k_{app} \times t \tag{9}$$

where k_{app} is the apparent rate constant of the first-order reaction (min^{-1}).

A plot of (Eq. (9)) is given in Fig. 8 it exhibits a straight line; the slope equals the apparent first-order rate constant k_{app}. Also, we determined the half-life value ($t_{1/2}$) of all films and the obtained values are listed in Table 3.

Fig. 8 shows that the best photocatalytic activities were found using CZO photocatalyst under UV light, with the rate constant (k_{app}) and half-time ($t_{1/2}$) of 0.011min^{-1} and 63 min respectively.

The kinetic study revealed that CZO thin film is a promising photocatalyst for the degradation of CV pollutant. Therefore, the photocatalytic stability of all ZnO was investigated by repeating the photodegradation measurements up to for three times. Fig. 9 shows the photodegradation efficiency of all films under UV and sunlight irradiations for 210 min after using them for three cycles. Indeed, under UV irradiation after three cycles, the photodegradation efficiencies are 73%, 81% and 71% for ZnO, CZO, and IZO respectively. Furthermore, under sunlight irradiation, the photodegradation efficiency achieved 68%; 79% and 82% for ZnO, CZO, and IZO respectively. The measurements clearly show that after three processes, the photo-degradation activity is slightly reduced (11%). Thus the investigated samples exhibit a negligible drop of their photocatalytic performances, suggesting that these films were reusable and retain good photodegradation efficiency. Moreover, this indicates a possibility for application of ZnO thin films as photocatalysts in wastewater treatments, mainly IZO under sunlight irradiation.

Table 3
Kinetic analysis: kinetic constants and $t_{1/2}$ of all ZnO thin films

Samples	$k_{app}(min^{-1})$	$t_{1/2}$(min)
ZnO (UV)	0.009	77
CZO (UV)	0.011	63
IZO (UV)	0.008	87
ZnO (sunlight)	0.007	99
CZO (sunlight)	0.008	86.6
IZO (sunlight)	0.009	77

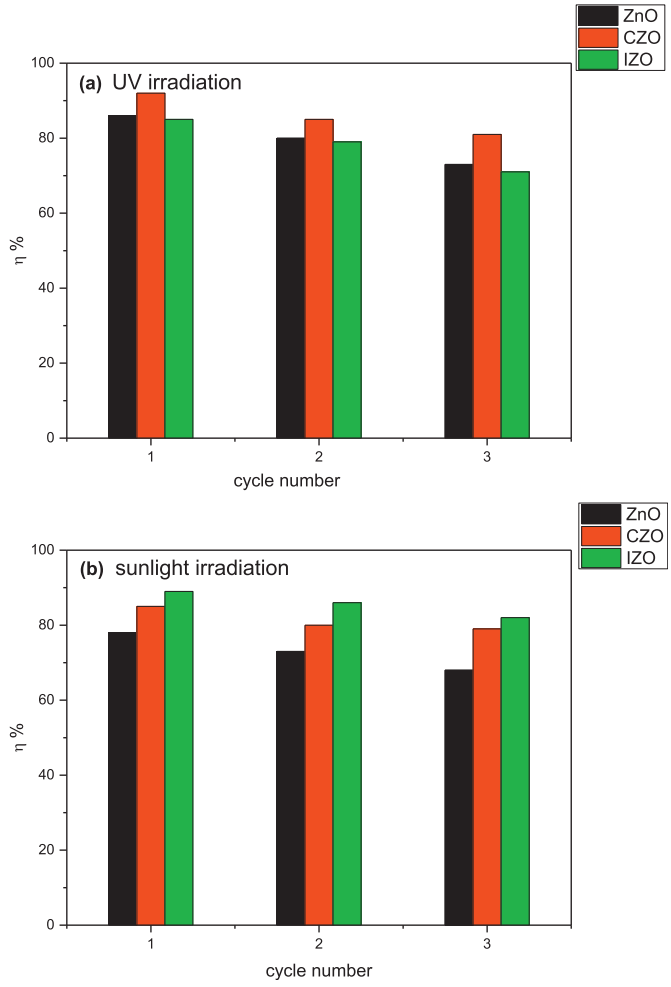

Fig. 9. The photodegradation efficiency through three consecutive photocatalysis versus cycle number: under (a) UV irradiation and (b) sunlight irradiation.

4. Conclusion

This work clearly shows a high photocatalytic performance of ZnO thin films deposited on PEI flexible substrate under either UV or sunlight irradiation. The effects of doping elements on photocatalytic activities of ZnO thin films are discussed. CZO thin films have higher photocatalytic activities under UV irradiation due to its good crystallinity combined with its high surface roughness. However, IZO has higher photocatalytic activities under sunlight irradiation due to its smaller band gap and its large specific area. In addition, all ZnO thin films retained high photodegradation efficiency even after three photocatalytic cycles, which is favorable for potential environmental and industrial applications. Furthermore, the obtained results confirm that ZnO thin films deposited on PEI flexible substrate are potential candidates as a photocatalyst for UV and solar photodegradation process of persistent organic pollutants. Besides, based on our investigations we can affirm that it is possible and easy to synthesize ZnO thin films on PEI flexible substrate (ZnO/PEI) as talented photocatalysts for applications in large surfaces with various geometries for photodegradation of hazardous pollutants.

Declarations

Author contribution statement

Samir Guermazi: Conceived and designed the experiments; Analyzed and interpreted the data; Contributed reagents, materials, analysis tools or data; Wrote the paper.

Hajer Guermazi: Conceived and designed the experiments; Analyzed and interpreted the data; Wrote the paper.

Mosbah Amlouk: Conceived and designed the experiments; Contributed reagents, materials, analysis tools or data; Wrote the paper.

Sameh Ben Ameur: Performed the experiments; Analyzed and interpreted the data; Wrote the paper.

Haythem Belhadj Ltaief: Performed the experiments; Analyzed and interpreted the data.

Benoit Duponchel: Performed the experiments; Analyzed and interpreted the data; Contributed reagents, materials, analysis tools or data.

Gérard Leroy: Conceived and designed the experiments; Analyzed and interpreted the data; Wrote the paper.

Funding statement

This work was supported by Tunisian Ministry of High Education and Scientific Research.

Competing interest statment

The authors declare no conflict of interest.

Additional information

No additional information is available for this paper.

Acknowledgements

Authors gratefully thank the financial support of the Tunisian Ministry of High Education and Scientific Research.

References

[1] A.P. Subramanian, S.K. Jaganathan, A. Manikandan, K.N. Pandiaraj, N. Gomathi, E. Supriyanto, Recent trends in nano-based drug delivery systems for efficient delivery of phytochemicals in chemotherapy, RSC Adv. 6 (2016) 48294–48314.

[2] A. Godlyn Abraham, A. Manikandan, E. Manikandan, S.K. Jaganathan, A. Baykal, P. Sri Renganathan, Enhanced opto-magneto properties of $Ni_x Mg_{1-x} Fe_2O_4$ ($0.0 \leq x \leq 1.0$) ferrites nano-catalysts, J. Nano. Opto. 12 (2017) 1326–1333.

[3] B. Meenatchi, V. Renuga, A. Manikandan, Size-controlled synthesis of chalcogen and chalcogenide nanoparticles using protic ionic liquids with imidazolium cation, Korean J. Chem. Eng. 33 (2016) 934–944.

[4] T. Hisatomi, J. Kubota, K. Domen, Recent advances in semiconductors for photocatalytic and photo electrochemical water splitting, Chem. Soc. Rev. 43 (2014) 7520–7535.

[5] G. Thennarasu, A. Sivasamy, Metal ion doped semiconductor metal oxide nanosphere particles prepared by soft chemical method and its visible light photocatalytic activity in degradation of phenol, Powder Technol. 250 (2013) 1–12.

[6] K. S Siddhapara, D.V. Shah, Study of photocatalytic activity and properties of transition metal ions doped nanocrystalline TiO2 prepared by sol-gel method, Ann. Mater. Sci. Eng. (2014).

[7] K. Kumar, M. Chitkara, I.S. Sandhu, D. Mehta, S. Kumar, Photocatalytic, optical and magnetic properties of Fe-doped ZnO nanoparticles prepared by chemical route, J. Alloy. Comp. 588 (2014) 681–689.

[8] J. Mazloom, F.E. Ghodsi, H. Golmojdeh, Synthesis and characterization of vanadium doped SnO_2 diluted magnetic semiconductor nanoparticles with enhanced photocatalytic activities, J. Alloy. Comp. 639 (2015) 393–399.

[9] N. Selvam, C. Sagaya, Manikandan, A. Kennedy, L. John, Vijaya, J. Judith, Comparative investigation of zirconium oxide (ZrO_2) nano and microstructures for structural, optical and photocatalytic properties, J. Colloid Interface Sci. 389 (2013).

[10] A. Manikandan, M. Durka, K. Seevankan, S. Arul Antony, A novel one-pot combustion synthesis and opto-magnetic properties of magnetically separable spinel $MnxMg_{1-x}fe_2O_4$ ($0.0<x<0.5$) nanophotocatalysts, J. Supercond. Nov. Magnetism 28 (2015) 1405–1416.

[11] T. Adachi, Sanjay S. Latthe, Suresh W. Gosavi, Nitish Roy, N. Suzuki, H. Kazuki Kato, Ken-ichi Katsumata, Kazuya Nakata, Manabu Furudate, Tomohiro Inoue, Takeshi Kondo, Makoto Yuasa, Akira Fujishima, Ch. Terashima, Photocatalytic, superhydrophilic, self-cleaning TiO_2 coating on cheap, light-weight, flexible polycarbonate substrates, Appl. Surf. Sci. 458 (2018) 917–923.

[12] K. Qi, B. Cheng, J. Yu, W. Ho, A review on TiO_2-based Z-scheme photocatalysts, Chin. J. Catal. 38 (2017) 1936–1955.

[13] S. Wang, B. Zhu, M. Liu, L. Zhang, J. Yu, M. Zhou, Direct Z-scheme ZnO/CdS hierarchical photocatalyst for enhanced photocatalytic H_2-production activity, Appl. Catal. B Environ. 243 (2019) 19–26.

[14] A.M. Ali, E.A.C. Emanuelsson, D.A. Patterson, Photocatalysis with nanostructured zinc oxide thin films: the relationship between morphology and photocatalytic activity under oxygen limited and oxygen rich conditions and evidence for a Mars Van Krevelen mechanism, Appl. Catal. B Environ. 97 (2010) 168–181.

[15] S.K. Pardeshi, A.B. Patil, Effect of morphology and crystallite size on solar photocatalytic activity of zinc oxide synthesized by solution free mechanochemical method, J. mol. catal. A-chem. 308 (2009) 32–40.

[16] K. Yogendra, S. Naik, K.M. Mahadevan, N. Madhusudhana, A comparative study of photocatalytic activities of two different synthesized ZnO composites against Coralene red F3BS dye in presence of natural solar light, J. Environ. Sci. Res. 1 (2011) 5–11.

[17] P. Georgiev, N. Kaneva, A. Bojinova, K. Papazova, K. Mircheva, K. Balashev, Effect of gold nanoparticles on the photocatalytic efficiency of ZnO films, Colloids Surf., A: Phychem. Eng. Asp 460 (2014) 240–247.

[18] A. Vijaya Manikandan, J. Judith Narayanan, S. Kennedy, L. John, Comparative investigation of structural, optical properties and dye-sensitized solar cell applications of ZnO nanostructures, J. Nanosci. Nanotechnol. 14 (2014) 2507–2514.

[19] A. Vijaya Manikandan, J. Judith Ragupathi, C. Kennedy, L. John, Optical properties and dye-sensitized solar cell applications of ZnO nanostructures prepared by microwave combustion synthesis, J. Nanosci. Nanotechnol. 14 (2014) 2584–2590.

[20] V. Sumithra, A. Manikandan, M. Durka, Saravana Kumar Jaganathan, A. Dinesh, N. Ramalakshmi, S. Arul Antony, Simple precipitation synthesis, characterization and antibacterial activity of Mn-doped ZnO nanoparticles, Adv. Sci. Eng. Med. 9 (2017) 483–488.

[21] G. Poongodi, R.M. Kumar, R. Jayavel, Structural, optical and visible light photocatalytic properties of nanocrystalline Nd doped ZnO thin films prepared by spin coating method, Ceram. Int. 41 (2015) 4169–4175.

[22] M.Sh. Abdel-wahab, A. Jilani, I.S. Yahia, Attieh A. Al-Ghamdi, Enhanced the photocatalytic activity of Ni-doped ZnO thin films: morphological, optical and XPS analysis, Superlattice. Microst. 94 (2016) 108–118.

[23] K. Qi, B. Cheng, J. Yu, W. Ho, Review on the improvement of the photocatalytic and antibacterial activities of ZnO, J. Alloy. Comp. 727 (2017) 792–820.

[24] Kai Ding, Wei Wang, Wei Wang, Dan Yu, Wei Wang, Pin Gao, Baojiang Li, Facile formation of flexible Ag/AgCl/polydopamine/cotton fabric composite photocatalysts as an efficient visible-light photocatalysts, Appl. Surf. Sci. 454 (2018) 101–111.

[25] J. Fu, B. Zhu, W. You, M. Jaroniec, J. Yu, A flexible bioinspired H_2-production photocatalyst, Appl. Catal. B Environ. 220 (2018) 148–160.

[26] Alessandro Di Mauro, Maria Elena Fragalà, Vittorio Privitera, Giuliana Impellizzeri, ZnO for application in photocatalysis: from thin films to nanostructures, Mater. Sci. Semicond. Process. 69 (2017) 44–51.

[27] S. Ben Ameur, H. Bel hadjltaief, A. Barhoumi, B. Duponchel, G. Leroy, M. Amlouk, H. Guermazi, Physical investigations and photocatalytic activities on ZnO and SnO_2 thin films deposited on flexible polymer substrate, Vacuum 155 (2018) 546–552.

[28] S. Ben Ameur, A. Barhoumi, H. Belhadjltaief, R. Mimouni, B. Duponchel, G. Leroy, M. Amlouk, H. Guermazi, Physical investigations of undoped and Fluorine doped SnO2 nanofilms on flexible substrate along with wettability and photocatalytic activity tests, Mater. Sci. Semicond. Process. 61 (2017) 17–26.

[29] P. Jongnavakit, P. Amornpitoksuk, S. Suwanboon, N. Ndiege, Preparation and photocatalytic activity of Cu-doped ZnO thin films prepared by the sol-gel method, Appl. Surf. Sci. 258 (20) (2012) 8192–8198.
[30] Zhao-Jin Wu, Wei Huang, Ke-Ke Cui, Zhi-Fang Gao, Ping Wang, Sustainable synthesis of metals-doped ZnO nanoparticles from zinc-bearing dust for photodegradation of phenol, J. Hazard Mater. 278 (2014) 91–99.
[31] N.V. Kaneva, D.T. Dimitrov, C.D. Dushkin, Effect of nickel doping on the photocatalytic activity of ZnO thin films under UV and visible light, Appl. Surf. Sci. 257 (18) (2011) 8113–8120.
[32] Y. Lu, Y. Lin, D. Wang, L. Wang, T. Xie, T. Jiang, A high performance cobalt-doped ZnO visible light photocatalyst and its photogenerated charge transfer properties, Nano. Res. 4 (11) (2011) 1144–1152.
[33] W. Yu, J. Zhang, T. Peng, New insight into the enhanced photocatalytic activity of N-, C- and S-doped ZnO photocatalysts, Appl. Catal. B Environ. 181 (2016) 220–227.
[34] M. Nolan, J. Hamilton, S. O'Brien, G. Bruno, L. Pereira, E. Fortunato, R. Martins, I. Povey, M. Pemble, The characterisation of aerosol assisted CVD conducting, photocatalytic indium doped zinc oxide films, J. Photochem. Photobiol. A Chem. 219 (1) (2011) 10–15.
[35] S. Ben Ameur, A. Barhoumi, R. Mimouni, M. Amlouk, H. Guermazi, Low-temperature growth and physical investigations of undoped and (In, Co) doped ZnO thin films sprayed on PEI flexible substrate, Superlattice. Microst. 84 (2015) 99–112.
[36] A. Boukhachem, B. Ouni, M. Karyaoui, A. Madani, R. Chtourou, M. Amlouk, Structural, opto-thermal and electrical properties of ZnO: Mo sprayed thin films, Mater. Sci. Semicond. Process. 15 (2012) 282–292.
[37] H. Bel Hadjltaief, S. Ben Ameur, P. Da Costa, M. Ben Zina, M.E. Gálvez, Photocatalytic decolorization of cationic and anionic dyes over ZnO nanoparticle immobilized on natural Tunisian clay, Appl. Clay Sci. 152 (2018) 148–157.
[38] H. Bel Hadjltaief, M. Ben Zina, M.E. Galvez, P. Da Costa, Photocatalytic degradation of methyl green dye in aqueous solution over natural clay-supported ZnO–TiO_2 catalysts, J. Photochem. Photobiol., A 315 (2016) 25–33.
[39] O. Bechambi, M. Chalbi, W. Najjar, S. Sayadi, Photocatalytic activity of ZnO doped with Ag on the degradation of endocrine disrupting under UV irradiation and the Investigation of its antibacterial activity, Appl. Surf. Sci. 347 (2015) 414–420.
[40] K.T. Ramakrishna Reddy, V. Supriya, Y. Murata, M. Sugiyama, Effect of Co-doping on the properties of Zn1-xCoxO films deposited by spray pyrolysis, Surf. Coating. Technol. 231 (2013) 149–152.
[41] M. Maria Lumina Sonia, S. Anand, V. Maria Vinosel, M. Asisi Janifer, S. Pauline, A. Manikandan, Effect of lattice strain on structure, morphology and magneto-dielectric properties of spinel NiGdxFe2−xO4ferrite nano-crystallites synthesized by sol-gel route, J. Magn. Magn. Mater. 466 (2018) 238–251.
[42] S. Asiri, S. Guner, A. Demir, A. Yildiz, A. Maznikandan, A. Baykal, Synthesis and magnetic characterization of Cu substituted barium hexaferrites, J. Inorg. Organomet. Polym. 28 (2018) 1065–1071.
[43] O.A. Yildirim, H. Arslan, S. Sönmezoğlu, Facile synthesis of cobalt-doped zinc oxide thin films for highly efficient visible light photocatalysts, Appl. Surf. Sci. 390 (2016) 111–121.
[44] P. Bindu, Sabu Thomas, Estimation of lattice strain in ZnO nanoparticles: X-ray peak profile analysis, J. Theor. Appl. Phys. 8 (2014) 123–134.
[45] P. Singh, Deepak, R.N. Goyal, A.K. Pandey, D. Kaur, Intrinsic magnetism in Zn1_xCoxO ($0.03< x < 0.10$) thin films prepared by ultrasonic spray pyrolysis, J. Phys. Condens. Matter 20 (1–6) (2008) 315005.
[46] S. Ilican, Y. Caglar, M. Caglar, B. Demirci, Polycrystalline indium-doped ZnO thin films: preparation and characterization, J.Opto. Adv. Mater. 10 (2008) 2592–2598.
[47] J. Gubicza, J. Szépvolgyi, I. Mohai, L. Zsoldos, T. Ungár, Particle size distribution and dislocation density determined by high resolution X-ray diffraction in nanocrystalline silicon nitride powders, Adv. Mater. Res. Switz. A280 (2000) 263–269.
[48] O. Belahssen, H. Ben Temam, S. Lakel, B. Benhaoua, S. Benramache, S. Gareh, Effect of optical gap energy on the Urbach energy in the undoped ZnO thin films, Optik 126 (2015) 1487–1490.
[49] A. Janotti, C.G. Van de Walle, Native point defects in ZnO, Phys. Rev. B 76 (16) (2007) 165–202.
[50] H. Zeng, G. Duan, Y. Li, S. Yang, X. Xu, W. Cai, Blue luminescence of ZnO nanoparticles based on non-equilibrium processes: defect origins and emission controls, Adv. Funct. Mater. 20 (4) (2010) 561–572.
[51] Z. Liang, Yu Xiang, B. Lei, P. Liu, W. Mai, Novel blue–violet photoluminescence from sputtered ZnO thin films, J. Alloy. Comp. 509 (2011) 5437–5440.
[52] H.B. Zeng, G.T. Duan, Y. Li, S.K. Yang, X.X. Xu, W.P. Cai, Blue luminescence of ZnO nanoparticles based on non-equilibrium processes: defect origins and emission control, Adv. Funct. Mater. 20 (2010) 561–572.
[53] Y.W. Heo, D.P. Norton, S.J. Pearton, Origin of green luminescence in ZnO thin film grown by molecular-beam epitaxy, J. Appl. Phys. 98 (7) (2005), 073502.
[54] R. Mimouni, A. Souissi, A. Madouri, K. Boubaker, M. Amlouk, High photocatalytic efficiency and stability of chromium-indium codoped ZnO thin films under sunlight irradiation for water purification development purposes, Curr. Appl. Phys. 17 (8) (2017) 1058–1065.
[55] C.-J. Chang, et al., Ce-doped ZnO nanoparticles for efficient photocatalytic degradation of direct red-23 dye, J. Solid State Chem. 214 (2014) 101–107.
[56] Yu-Cheng Chang, Pei-Shih Lin, Fu-Ken Liu, Jin-You Guo, Chien-Ming Chen, One-step and single source synthesis of Cu-doped ZnO nanowires on flexible brass foil for highly efficient field emission and photocatalytic applications, J. Alloys Comp. 688 (2016) 242–251.
[57] J. Rashid, M.A. Barakat, N. Salah, S.S. Habib, ZnO-nanoparticles thin films synthesized by RF sputtering for photocatalytic degradation of 2-chlorophenol in synthetic wastewater, J. Ind. Eng. Chem. 23 (2015) 134–139.
[58] P.M. Perillo, M.N. Atia, C-doped ZnO nanorods for photocatalytic degradation ofp-aminobenzoic acid under sunlight, Nano-Struct. Nano-Objects 10 (2017) 125–130.
[59] R. Kumar, Umar Ahmad, G. Kumar, M.S. Akhtar, Yao Wang, S.H. Kim, Ce-doped ZnO nanoparticles for efficient photocatalytic degradation of direct red-23 dye, Ceram. Int. 41 (2015) 7773–7782.
[60] X. Qiu, L. Li, J. Zheng, J. Liu, X. Sun, G. Li, Origin of the enhanced photocatalytic activities of semiconductors: a case study of ZnO doped with Mg^{2+}, J. Phys. Chem. C 112 (2008) 12242–12248.
[61] Ozlem Altintas Yildirim, Hanife Arslan, Savas Sonmezoğlu, Facile synthesis of cobalt-doped zinc oxide thin films for highly efficient visible light photocatalysts, Appl. Surf. Sci. 390 (2016) 111–121.
[62] M.H. Huang, Y. Wu, H. Feick, N. Tran, E. Weber, P. Yang, Catalytic growth of zinc oxide nanowires by vapor transport, Adv. Mater. 13 (2001) 113–116.
[63] Q. Tang, W. Zhou, J. Shen, W. Zhang, L. Kong, Y. Qian, A template-free aqueous route to ZnO nanorod arrays with high optical property, Chem. Commun. 21 (2004) 712–713.
[64] L. Xu, Y.L. Hu, C. Pelligra, C.H. Chen, L. Jin, H. Huang, S. Sithambaram, M. Aindow, R. Joesten, S.L. Suib, ZnO with different morphologies synthesized by solvothermal methods for enhanced photocatalytic activity, Chem. Mater. 21 (2009) 2875–2885.